Comparative Channel Study of Ray Tracing and Measurement for an Indoor Scenario at 28 GHz

Jinnan Zhan[1], Jianhua Zhang[2], Lei Tian[1], Xinzhuang Zhang[1], Pan Tang[1], Jianwu Dou[3], Hewen Wei[4]
[1]Key Lab of Universal Wireless Communications, Ministry of Education,
[2]State Key Lab of Networking and Switching Technology,
Beijing University of Posts and Telecommunications, Mailbox NO.92, 100876, Beijing, China
[3]Wireless Algorithm Department, Product R&D system, ZTE Corp. Ltd., 201210, Shanghai, China
[4]National Key Laboratory of Science and Technology on Blind Signal Processing, 610041, Chengdu, Sichuan, China
Email: {zjn1994, jhzhang, tianlbupt}@bupt.edu.cn;{dou.jianwu}@zte.com.cn

***Abstract*—The millimeter wave communication is important for future wireless systems. In this paper, the channel characteristics at 28 GHz in an indoor scenario are researched based on ray tracing (RT) simulation and measurement. In the RT simulation, various configurations, such as different number of reflections, diffractions and penetrations are used. As for the measurement, two setups are implemented in order to analyze more parameters. Setup one is that biconical antennas are used at both the transmitter (TX) and receiver (RX). The other setup is that horn antenna at RX is rotated 360° in azimuth with a step of 5° when an omni-directional antenna located at TX. Meanwhile, antenna is rotated one circle with an elevation angle of 10°, 0° and -10°, respectively. Path loss and K-factor are analyzed firstly, and analysis results indicate the RT result with 1 or 2 reflections, 1 diffractions and 5 penetrations in this conference room is closest to the measurement result and channel models in 3GPP TR 38.901. Then, the root mean square (RMS) delay spread and RMS angular spread are investigated, which shows the value of measurement is a bit larger than RT because of the limitation of azimuth and elevation step. According to all the results, 1-2 reflections, 1 diffraction and 5 penetrations can be used in RT for future analysis of indoor scenario at 28 GHz.**

***Index Terms*—ray tracing, channel measurement, mm-wave, indoor, 28 GHz.**

I. Introduction

In order to address the high requirements of data rate and system capacity, various committees and groups contribute to the research on millimeter wave (mm-wave) for fifth generation (5G) [1], [2]. Mm-wave channel characteristics are obtained by channel sounding system with high-directivity antennas [1]–[4]. However, since the narrow-beam antennas need to be rotated over all azimuth-elevation pairs to capture complete channel characteristics in the spatial domain, the time consumption and system complexity of the measurements drastically increases. To overcome this problem, deterministic channel model based on ray tracing (RT) simulations, which can predict deterministic propagation, has became pivotal [4]. While the scatterers of indoor scenario are complex and limited, RT is very attractive due to the high precision requirements.

According to recent literature, the channel can be represented by the combination of several paths originating from line-of-sight (LoS), specular reflection, and diffraction which may cause propagation and penetration loss in a certain scenario [4]–[7]. In [4], the dynamic channel characteristics at 23.5 GHz in an indoor scenario are investigated according to measurement and deterministic simulation. [5] compares measurements and RT results at two indoor scenarios, a large unfurnished basement and a small furnished indoor office, at 26-30 GHz. Angle-of-arrivals and delay-of-arrivals of the multipath components are mainly analyzed. [6] draws conclusions on path loss, delay spread (DS), and angular spread (AS) at both 28 GHz and 3.5 GHz by using RT only. All of above research results have preset RT parameters based on experience before comparisons, such as the number of reflections, number of diffractions and number of penetrations. In [7], the choice of these RT parameters are discussed and the accuracy of RT predictions is examined. The results are drawn by comparing path loss and root mean square (RMS) DS. However the spatial parameters such as angle of arrivals have not been studied currently. In this paper, path loss, K-factor, RMS DS and RMS AS are analyzed between RT and measurement by setting up various RT parameters.

The rest of this paper is organized as follow. In Section II, the data acquisitions based on measurement and RT simulation are described. The analyses of path loss, K-factor, RMS DS and RMS AS are compared in Section III. Finally, conclusions are given in Section IV to summarize the whole work.

II. Data Acquisition

A. Measurement Campaign

The panorama of the environment is presented in Fig.1(a). And this is a typical furnished indoor conference scenario with the geometric size equaling to $10.97 \times 6.62 \times 2.40$ m^3. Fig.1(b) shows TX was fixed at a corner of room whereas 16 measuring positions were distributed in various locations in the room. Besides, the same height 1.55m above the ground was chosen for both TX as well as RX.

The measurement campaign was carried out based on a correlator channel sounder with 600 MHz bandwidth at 28 GHz. Transmitter and receiver were synchronized by the same reference clock source. In order to achieve greater dynamic range in the link budget, the power amplifier and low noise amplifier (LNA) were used at TX and RX respectively [1].

(a) The panorama of the indoor measurement environment.

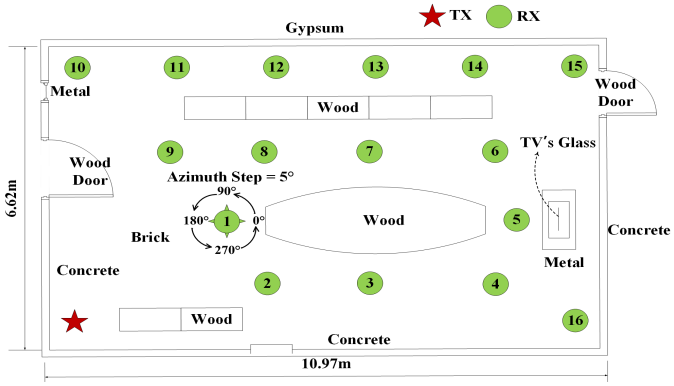

(b) Measurement environment layout.

Fig. 1. Detailed exhibition of measurement environment.

For each measuring position, measurement was divided into two parts by different setups.

1) Setup One: Biconical antennas (5.2 dBi) were used at both TX and RX in order to collect all multipath components (MPCs) information.

2) Setup Two: Rotating the horn antenna (25 dBi, 10° HPBW, 11° EPBW) at RX over azimuth-elevation pairs successively while an omni-directional antenna (2.93 dBi) is used at TX. At the elevation angle of 10°, 0° and -10°, the receiver acquired 72 samples at each circle while the rotating step is 5°. Therefore, most paths from different directions could been recorded independently and the spatial domain parameters can be analyzed. The key configurations of setup two are listed in Table I as a summary.

TABLE I
28GHz MEASUREMENT CONFIGURATIONS OF SETUP TWO

Parameter	Value
TX Antenna	Omni-directional
RX Antenna	Horn
Ant.Polarization	V-to-V
RX Azimuth Angle	0°-360°(step = 5°)
RX Elevation Angle	10°,0°,-10°(step = 10°)

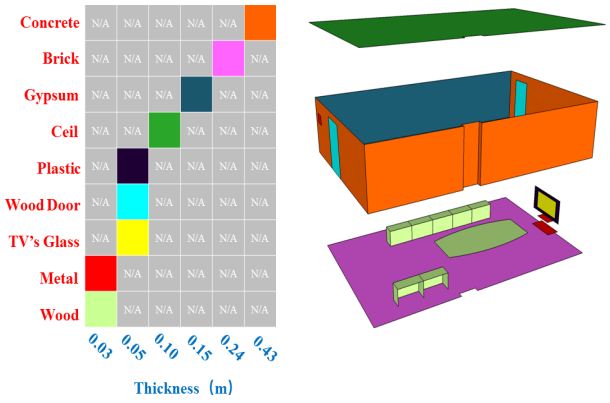

Fig. 2. Digitized map for the measurement scenario.

B. Ray Tracing Simulation

A full 3D ray tracing (RT) software developed by ZTE and Beijing University of Posts and Telecommunications (BUPT) was used in this research. Three main steps are introduced to generate the channel realizations in the specified scenario, i.e., constructing the detailed 3D digital map, calculating the geometric parameters for each propagation path and implementing the electromagnetic calculations according to propagation mechanisms, such as direct LoS, specular reflection and diffraction [4].

Fig.2 shows the digitalized map of the measurement scenario. The freely available 3D modeling software Google Sketch Up has been used for building it. Different kinds of materials are color-coded according to the legend, which can be distinguished by the RT software. The corresponding electromagnetic properties (i.e., relative permittivity and conductivity) at specified frequency are adopted depending on the ITU deliverable [8].

Considering the uncertainty of the comparison results, various configurations have been simulated such as different number of reflections, diffractions and penetrations. The other configurations of RT, such as transmit power and antenna radiation patterns, are same as the measurement.

The examples of the RT simulations results are presented in Fig.3. It shows all the propagation paths from TX to No.6 RX with different number of reflections. “2 Ref” in the title represents that reflection paths are not more than 2 reflections, which means that the figure contains paths of 1 reflection and 2 reflections. “1 Dif” means there are 1 diffraction paths. Accordingly, “5 Pe” represents that there would not be paths encountering more than 5 penetrations. Fig.3(a) shows that there are 1 path of LoS, 9 paths of 1 reflection, 29 paths of 2 reflections and 11 paths of 1 diffraction. Meanwhile, all 50 paths penetrate less than 5 objects. Compared to Fig.3(a), Fig.3(b) has more paths due to 72 paths of 3 reflections.

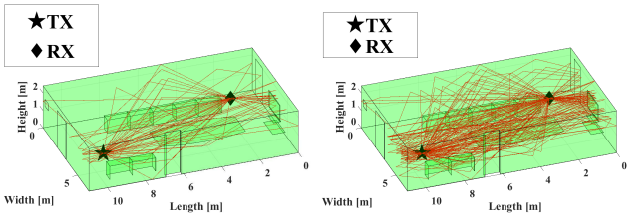

(a) 2 Ref, 1 Dif and 5 Pe. (b) 3 Ref, 1 Dif and 5 Pe.

Fig. 3. The propagation paths from TX to No.6 RX with different configurations.

III. Result Comparison

A. Path Loss

Close-in (CI) model of path loss (PL) model has been applied in [9]. It is given by (1):

$$PL^{CI}(f,d)[dB] = FSPL(f,1\ m)[dB] + 10nlog_{10}(d) + \chi_{\sigma}^{CI}, where\ d \geq 1\ m \quad (1)$$

where n denotes the single model parameter, the path loss exponent (PLE), d is the 3D T-R separation distance, and $FSPL(f,1\ m) = 20log_{10}(\frac{4\pi f}{c})$ denotes the free space path loss in dB at a T-R separation distance of 1 m at the carrier frequency f, where c is the speed of light. And χ_{σ}^{CI} is the shadow fading (SF) standard deviation describing large-scale signal fluctuations about the mean path loss over distance [9].

PL in RT can be expressed as:

$$PL_{RT,i} = P_{T,i} + G_{A,i} - \sum_{r=1}^{N} P_{r,i} \quad (2)$$

where $P_{T,i}$, $G_{A,i}$ and $P_{r,i}$ represent transmitting power, antenna gains and the rth path power of ith RX (r = 1, 2, $\cdots$, N).

PL comparisons of RT and measurement are shown in Fig.4. The "Ref", "Dif" and "Pe" in the legend means reflections, diffractions and penetrations.

Firstly, the effect of number of reflections on PL is investigated in Fig.4(a). Meanwhile, the number of diffractions is 0 while number of penetrations is 5. "0 Ref" means there is only direct LoS path in RT. Its value is slightly lower than the free space loss while trend keeps consistent. PL in RT reduces by almost 3 dB with the increase of number of reflections at 10.5-meter position which is the distance from TX and No.15 RX. Meanwhile, the value gradually approaches the measured value. After 2 Ref, PL is almost the same even if number of reflections keep increasing. 1.5 dB gap between RT and measurement results may arise from that the 3D modeling for this room is not absolutely accurate. Another reason can be the LNA of measurement, whose error range is about 1 dB at 28 GHz.

Secondly, the effect of diffractions is studied in Fig.4(b). The case is compared when 2 Ref and 5 Pe. PL has a slight change when the number of diffraction changes from 0 to 1,

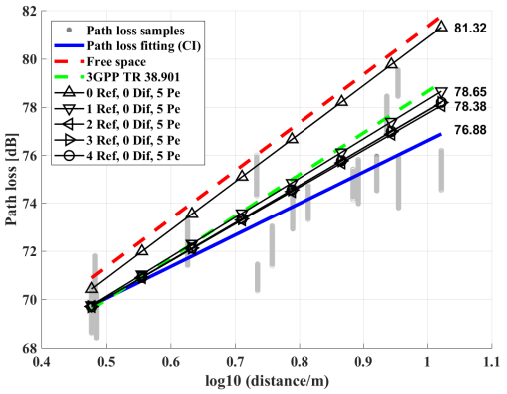

(a) RT (different number of reflections) vs. Measurement.

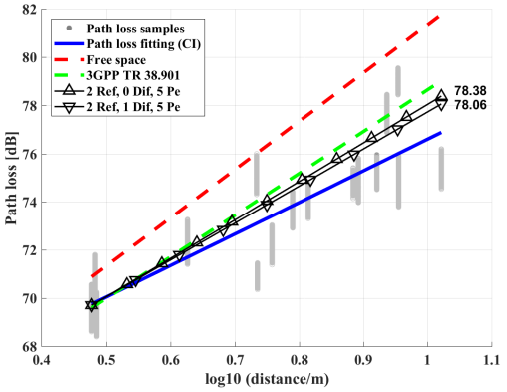

(b) RT (different number of diffractions) vs. Measurement.

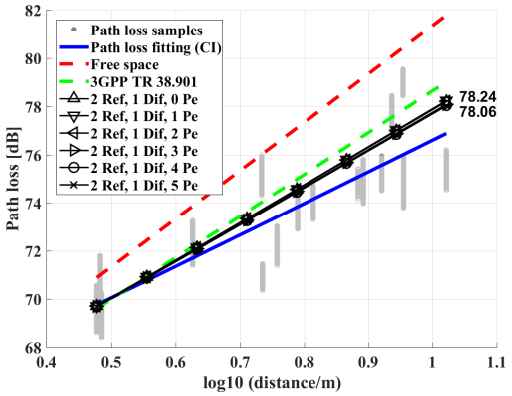

(c) RT (different number of penetrations) vs. Measurement.

Fig. 4. Path loss comparisons of RT and measurement.

and the difference is 0.32 dB at the furthest distance between TX and RX. Although the impact of number of diffractions is relatively small, it is better to add it in RT in order to approximate the measured value.

Finally, Fig.4(c) indicates that increasing number of penetrations has little impact on PL when 2 Ref and 1 Dif. There are no obvious obstructions in this scenario except tables and TV that could be penetrated by paths, so that PL is almost

constant. The number of penetrations can be more important in RT if the scene is more complicated.

In conclusion, the higher configuration parameters are set, the closer RT value is to the measured value on PL . From another point of view, every additional number of reflections, time and storage costs are almost doubled. Increasing the number of diffractions and number of penetrations, the cost increases less. Therefore, 1 or 2 Ref, 1 Dif, more than 5 Pe can be accepted in PL analysis considering the cost of time and storage space.

B. K-factor

The Ricean K-factor is defined as the ratio of power of the direct LoS components to the other MPCs. It is obtained as

$$K_{Mea} = \frac{\sqrt{G_m^2 - G_v^2}}{G_m - \sqrt{G_m^2 - G_v^2}} \tag{3}$$

where G_m is the average power gain and G_v is the RMS fluctuation of power gain.

According to definition of Ricean K-factor, the K-factor of ith RX in RT can be expressed as

$$K_{RT,i} = \frac{P_{LoS,i}}{P_{All,i} - P_{LoS,i}} \tag{4}$$

where $P_{LoS,i}$ and $P_{All,i}$ are the power of direct LoS path and the power of all paths at ith RX.

TABLE II
K-FACTOR [dB]

K-factor	μ_K	δ_K
3GPP TR 38.901 (Indoor-Office)	3.3484	5.3418
Measurement	3.2358	3.8438
1 Ref, 0 Dif, 5 Pe	3.0230	1.6039
1 Ref, 1 Dif, 5 Pe	3.0230	1.6565
2 Ref, 1 Dif, 5 Pe	2.3527	1.4077
3 Ref, 1 Dif, 5 Pe	2.2566	1.3874

According to the results of the PL, the effect of penetration in this scenario is little so they would not be investigated here. Table II lists the results of K-factor in measurement and RT with different configuration parameters. From the table, it is found that the K-factor of 1 Ref, 0 or 1 Dif and 5 Pe is closest to measurement and 3GPP TR 38.901 [10]. When the number of reflections grows to 2 or more, its value is almost stable at a lower value.

For this phenomenon, denoising is the main reason. In order to ensure a reasonable signal to noise ratio (SNR), some low-power paths which are submerged in the noise are artificially removed in data processing of measurement. Meanwhile, these low-power paths are mainly composed of high-order reflections paths and diffraction paths. After denoising the measurement data, the power proportion of main component would be greater. Therefore, the mean of K-factor in measurement would always be larger than RT.

C. RMS Delay Spread

The main parameters characterizing delay dispersion are the mean excess delay τ_{mean} and RMS DS τ_{rms}. Assume that $p(r)$ indicates the power of the rth path in measurement and the power of the rth path in RT (r = 1, 2, $\cdots$, N). τ_r is the delay of the rth path in measurement and the delay of the rth path in RT. So the RMS DS is defined as in the following.

$$\tau_{rms} = \sqrt{\frac{\sum_{r=1}^{N}(\tau_r - \tau_{mean})^2 \cdot p(r)}{\sum_{r=1}^{N} p(r)}} \tag{5}$$

where

$$\tau_{mean} = \frac{\sum_{r=1}^{N} \tau_r \cdot p(r)}{\sum_{r=1}^{N} p(r)} \tag{6}$$

TABLE III
RMS DELAY SPREAD [lg10(DS/1s)]

RMS Delay Spread	μ_{lgDS}	δ_{lgDS}
3GPP TR 38.901 (Indoor-Office)	-7.8046	0.2660
Measurement	-8.0046	0.1756
1 Ref, 0 Dif, 5 Pe	-8.4783	0.2523
1 Ref, 1 Dif, 5 Pe	-8.4783	0.2605
2 Ref, 1 Dif, 5 Pe	-8.2442	0.1156
3 Ref, 1 Dif, 5 Pe	-8.1643	0.1019
4 Ref, 1 Dif, 5 Pe	-8.1285	0.0953

Table III compares RMS DS obtained from measurement and RT. The RMS DS obtained from measurement are smaller than that in 3GPP TR 38.901 because of smaller experimental scenario. With the increase in the number of reflections in the RT, the value are gradually approaching the measured value.

The reason for this phenomenon is the actual measurement environment is more complex than RT 3D modeling. So that there are more unknown paths in measurement than RT. It can be expected that the RMS DS of RT would be closer to the measurement when the number of reflections is similar enough to the actual situation. However, 2 Ref in RT can characterize delay dispersion in measurement to a certain degree.

D. RMS Angular Spread

SAGE algorithm [3] is used to extract the parameters including azimuth angle of arrival (AoA), elevation angle of arrival (EoA) and power of paths from the measurement data with the setup two.. RT is simulated for 1 Dif and 5 Pe while different number of reflections. The cumulative distribution functions (CDFs) of RMS AS in azimuth (ASA) and elevation (ESA) planes are represented in Fig.5, respectively.

On the one hand, with the increase of the number of reflections in RT, RMS ASA in RT increases a bit then remains stable while RMS ESA in RT has barely changed. Meanwhile, 70% of locations encounter an ASA larger than 45° for both measurement and RT with 2 or more Ref. On the other hand,

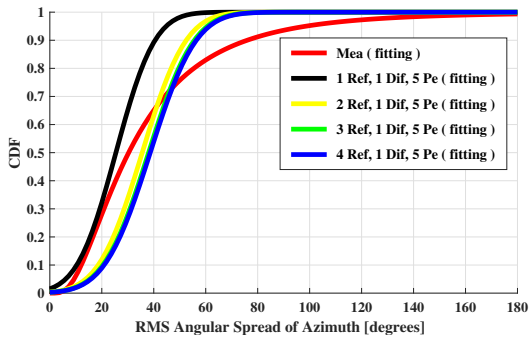

(a) CDF of RMS ASA.

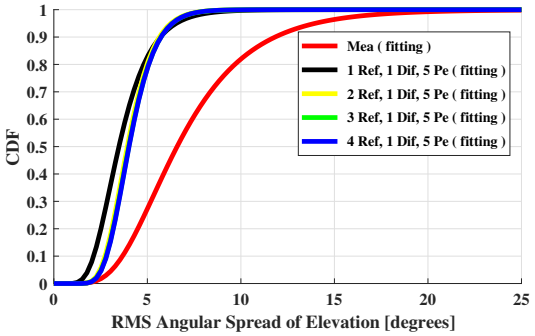

(b) CDF of RMS ESA.

Fig. 5. CDFs of RMS Angular Spread.

the mean of RMS ESA in measurement would not be less than 10° because of the effect of 10° elevation step. From the perspective of angle distribution, 2 Ref at least can be used for RT to keep similar to measurement.

More specific statistics are recorded in Table IV.

TABLE IV
RMS ANGULAR SPREAD [$lg10$(ASA *or* ESA/1°)]

RMS Angular Spread	μ_{lgASA}	δ_{lgASA}	μ_{lgESA}	δ_{lgESA}
3GPP TR 38.901	1.5821	0.1755	0.8298	0.1115
Measurement	1.4820	0.3110	0.8188	0.1983
1 Ref, 1 Dif, 5 Pe	1.3544	0.2299	0.5416	0.1667
2 Ref, 1 Dif, 5 Pe	1.5213	0.1695	0.5941	0.1225
3 Ref, 1 Dif, 5 Pe	1.5516	0.1666	0.6028	0.1208
4 Ref, 1 Dif, 5 Pe	1.5588	0.1658	0.6043	0.1200

IV. Conclusion

In this paper, the characteristics of the wireless channel at 28 GHz in an indoor conference room have been analyzed. The channel parameters, path loss, K-factor, RMS DS and RMS AS, have been researched based on RT simulation and measurement individually. For path loss, the effects of number of reflections, diffractions and penetrations in RT have been evaluated respectively. The result shows that the RT value gradually approaches the measured value with the increase of number of reflections however there would be almost unchanged more than 2 Ref. Although the number of diffractions and penetrations have little influence compared to reflections, the simulation can be more accurate by increasing them. It has been found that the K-factor of 1 Ref, 0 or 1 Dif and 5 Pe is closest to measurement and 3GPP TR 38.901. Moreover, the statistics of RMS DS and RMS AS have been observed. The higher number of reflections, the closer RMS DS and RMS AS of RT are to the measured values. However, RMS AS from RT would always be lower than measurement due to the influence of step in measurement. Taking into account the sharp rise in time and storage costs while increasing number of RT parameters, 1-2 Ref, 1 Dif and 5 Pe can be used in RT for future analysis of indoor scenario at 28 GHz.

Acknowledgment

The research is supported by National Science and Technology Major Project of the Ministry of Science and Technology (2017ZX03001012-003), and by The Ministry of Education-China Mobile Research Fund with MCM20160105, and by National Natural Science Foundation of China and project with NO. 61322110, and by Exploratory Project of State Key Lab of Networking and Switching Technology (NST20170205), and the authors would like to thank ZTE.

References

[1] J. Zhang, P. Tang, L. Tian, Z. Hu, T. Wang, and H. Wang, "6–100 GHz research progress and challenges from a channel perspective for fifth generation (5G) and future wireless communication," *SCIENCE CHINA Information Sciences*, vol. 60, no. 8, pp. –, 2017.

[2] T. S. Rappaport, Y. Xing, G. R. MacCartney, A. F. Molisch, E. Mellios, and J. Zhang, "Overview of Millimeter Wave Communications for Fifth-Generation (5G) Wireless Networks-with a focus on Propagation Models," *IEEE Transactions on Antennas and Propagation*, vol. PP, no. 99, pp. 1–1, 2017.

[3] T. Jiang, L. Tian, P. Tang, Z. Hu, and J. Zhang, "Basestation 3-dimensional spatial propagation characteristics in urban microcell at 28 GHz," in *2017 11th European Conference on Antennas and Propagation (EUCAP)*, pp. 3167–3171, March 2017.

[4] N. Zhang, J. Dou, L. Tian, X. Yuan, X. Yang, S. Mei, and H. Wang, "Dynamic Channel Modeling for an Indoor Scenario at 23.5 GHz," *IEEE Access*, vol. 3, pp. 2950–2958, 2015.

[5] A. Karstensen, W. Fan, I. Carton, and G. F. Pedersen, "Comparison of ray tracing simulations and channel measurements at mmWave bands for indoor scenarios," in *2016 10th European Conference on Antennas and Propagation (EuCAP)*, pp. 1–5, April 2016.

[6] A. O. Kaya, D. Calin, and H. Viswanathan, "28 GHz and 3.5 GHz Wireless Channels: Fading, Delay and Angular Dispersion," in *2016 IEEE Global Communications Conference (GLOBECOM)*, pp. 1–7, Dec 2016.

[7] M. Peter, W. Keusgen, and R. Felbecker, "Measurement and Ray-Tracing Simulation of the 60 GHz Indoor Broadband Channel: Model Accuracy and Parameterization," in *The Second European Conference on Antennas and Propagation, EuCAP 2007*, pp. 1–8, Nov 2007.

[8] ITU-R P.1238-8, "Propagation Data and Prediction Methods for the Planning of Indoor Radiocommunication Systems and Radio Local Area Networks in the Frequency Range 300 MHz to 100 GHz," 2015.

[9] S. Sun, G. R. MacCartney, and T. S. Rappaport, "Millimeter-wave distance-dependent large-scale propagation measurements and path loss models for outdoor and indoor 5G systems," in *2016 10th European Conference on Antennas and Propagation (EuCAP)*, pp. 1–5, April 2016.

[10] 3GPP TR 38.901 V14.1.1, "Study on channel model for frequencies from 0.5 to 100 GHz (Release 14)," Technical report, 2017.